

ARTICLE

Size effects on dislocation starvation in Cu nanopillars : A molecular dynamics simulations study

G. Sainath^{a,b}, Vani Shankar^{a,b} and A. Nagesha^{a,b}

^aMechanical Metallurgy Division, Metallurgy and Materials Group, Indira Gandhi Centre for Atomic Research, Kalpakkam, Tamilnadu-603102, India

^bHomi Bhabha National Institute, Training School Complex, Anushaktinagar, Mumbai, Maharashtra-400094, India

ARTICLE HISTORY

Compiled October 4, 2023

ABSTRACT

Size plays an important role on the deformation mechanism of nanopillars. With decreasing size, many FCC nanopillars exhibit dislocation starvation state which is responsible for their high strength. However, many details about the dislocation starvation mechanism like how often it occurs, and how much is its contribution to the total plastic strain, are still elusive. Similarly, the size below which the dislocation starvation occurs in the nanopillars is not clearly established. In this context, the atomistic simulations have been performed on the compressive deformation of $\langle 110 \rangle$ Cu nanopillars with size (d) ranging from 5 to 21.5 nm. The molecular dynamics (MD) simulation results indicate that the nanopillars deform by the slip of extended dislocations and exhibit dislocation starvation mainly at small sizes (< 20 nm). The frequency of the occurrence of dislocation starvation is highest in small size nanowires and it decreases with increasing size. Above the nanopillar size of 20 nm, no dislocation starvation has been observed. Further, we define the dislocation starvation strain and based on this, it has been shown that, the contribution of dislocation starvation state to the total plastic strain decreases from 70% in small size nanopillars to below 5% in large size pillars. The present results suggest that the dislocation starvation is a dominant phenomena in small size nanopillars.

KEYWORDS

Nanopillars; Size effects; Dislocation starvation; Atomistic Simulations

1. Introduction

It is well known that the mechanical properties and associated plastic deformation behaviour of crystalline materials is mainly governed by the movement of partial or full dislocations and depends mainly on temperature and strain rate. In bulk materials, the yield stress and the plastic deformation mechanisms were independent of size. However, when the sample size is reduced to nanoscale, the mechanical properties along with plastic deformation mechanisms exhibit strong size dependence [1,2]. The high surface area to volume ratio and low density of defects provides the nanostructures with mechanical properties different from bulk single crystals. The plastic deformation in nanowires/nanopillars occurs either by dislocation slip or

twinning depending on the crystallographic orientation [3,4]. Many studies over the last two decades have suggested that the size also influence the operative deformation mechanisms [1,2,5,6]. Using in-situ transmission electron microscopy (TEM) experiments on Ag nanowires, a transition in deformation mechanisms has been reported with increasing size [6]. In Ag nanowires of 11 nm diameter, the deformation proceeds by the slip of full dislocations, while nucleation and annihilation of stacking faults has been observed in relatively smaller diameters in the range 5-8 nm. In sub 3 nm size nanowires, the deformation is accommodated by the relative slip between two adjacent glide planes without any dislocations [6]. Similarly, in-situ TEM experiments on gold revealed that thick films deformed predominantly by perfect dislocations, while thin films deformed mainly by partial dislocations separated by stacking faults [2]. Like deformation mechanism, the yield strength of FCC nanopillars also shows strong size dependence. The yield strength of nanowires/nanopillars increases with decreasing diameter and it is significantly higher than their bulk counterparts [1,5]. In order to explain this 'smaller is stronger' trend in nanopillars, the dislocation starvation has been proposed as one of the strengthening mechanisms in small size nanopillars [7]. The mechanism of dislocation starvation involves the continuous escape of dislocations to nearby free surfaces without any multiplication leading to a scarcity of dislocations in the nanopillar. This dislocation free state of the nanopillar during the plastic deformation is known as dislocation starvation state [7] or mechanical annealing [8]. This mechanism originates from the micro-structural parameters and dimensional constraints such as high stress and small size [9,10], which is readily satisfied in nanowires and nanofilms. Following dislocation starvation, the nanopillar deforms elastically until new dislocations nucleate to continue further plastic deformation. This continuous nucleation of dislocations requires high stress which leads to dislocation starvation hardening [10]. Experimentally, the dislocation starvation mechanism has been observed in many FCC nanowires, nanopillars and nanofilms [7,8,10,11].

Investigating the dislocation starvation related mechanism using conventional experimental methods is quite tedious and requires sophisticated instruments. In this context, computational methods based on molecular dynamics (MD) and dislocation dynamics (DD) simulations are adopted to understand the dislocation related behaviours in nanopillars [12–15]. The 3D DD simulation study by Zhou et al. [15] on Ni micropillars has revealed that the dislocation starvation at an early stage of plastic deformation was due to weakly entangled dislocations leaving the sample. The DD study by Greer et al. [12] and MD simulations study by Weinberger and Cai [13] have demonstrated that the dislocation starvation occurs only in FCC nanopillars and no dislocation starvation has been observed in BCC nanopillars. MD simulations study by Cao et al. [14] on Ni nanopillars of diameters ranging from 4 to 16 nm has revealed that in dislocation starvation state, the nanopillars deform elastically until new dislocations nucleate from the surfaces. Despite these experimental and simulation studies [7,8,10–15], many details about the dislocation starvation are still elusive. For example, how often the dislocation starvation occurs during the plastic deformation and what is the contribution of dislocation starvation to the total plastic strain is not investigated. Similarly, the nanopillar size limits below which the dislocation starvation occurs is not clearly established. In view of this, a systematic MD simulations have been performed on Cu nanopillars with size ranging from 5 to 21.5 nm to investigate the dislocation starvation mechanism under the compressive loading. The size dependence of dislocation starvation and its contribution to the total plastic strain have

been investigated in detail.

2. Simulation Details

All MD simulations have been carried out in Large scale Atomic/Molecular Massively Parallel Simulator (LAMMPS) package [16]. Embedded atom method (EAM) potential for Cu given by Mishin and co-workers [17] has been used for describing the inter-atomic forces between copper atoms. This EAM potential is widely used to study the plastic deformation related studies in Cu nanowires/nanopillars [18,19]. As shown in Figure 1, single crystal Cu nanopillars oriented in $[1\bar{1}0]$ axial direction with (111) and $(11\bar{2})$ as side surfaces were considered for this study. The $\langle 110 \rangle$ orientation is selected mainly because of its wide and ease of synthesis [20]. In the literature, it is widely synthesized orientation due to the preferential growth of Cu nanopillars along the $\langle 110 \rangle$ direction, where the $\{111\}$ planes are exposed to the surface, which have a lowest surface energy and hence stabilize the nanopillar [20]. The model nanopillars had a square cross section shape with a cross section width (d) ranging from 5 to 21.5 nm (Figure 1). The pillar length (l) was twice the cross section width (d). In order to mimic the nanopillar surfaces, no periodic boundary conditions were used in any direction. Similar boundary conditions were used for nanopillars in earlier studies [19,21,22]. The model system was equilibrated to a required temperature of 10 K in NVT ensemble. Upon completion of equilibrium process, the compressive loading is applied in a displacement controlled manner at a constant strain rate of $3.5 \times 10^8 \text{ s}^{-1}$ by imposing displacements to atoms along the loading axis ($[1\bar{1}0]$ axis) that varied linearly from zero at the bottom layer to the maximum value at the top layer [19,21,22]. For all the nanopillars, the compressive loading has been performed up to a strain level of 0.25. The average stress is calculated from the Virial expression [23]. In order to analyze the deformation, the visualization of atomic snapshots is accomplished using AtomEye [24]. The Burgers vector of dislocations were determined by dislocation extraction algorithm (DXA) [25] as implemented in OVITO [26] and were assigned according to Thomson tetrahedron.

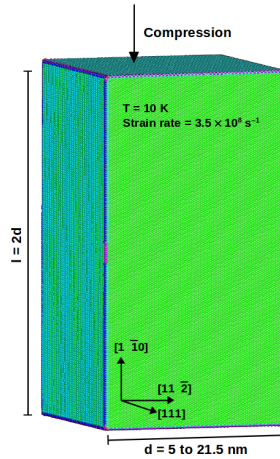


Figure 1.: The initial structure of the Cu nanopillar considered in this study. It contains the details of orientation, size, length or aspect ratio and loading direction. The atoms are coloured according to their potential energy.

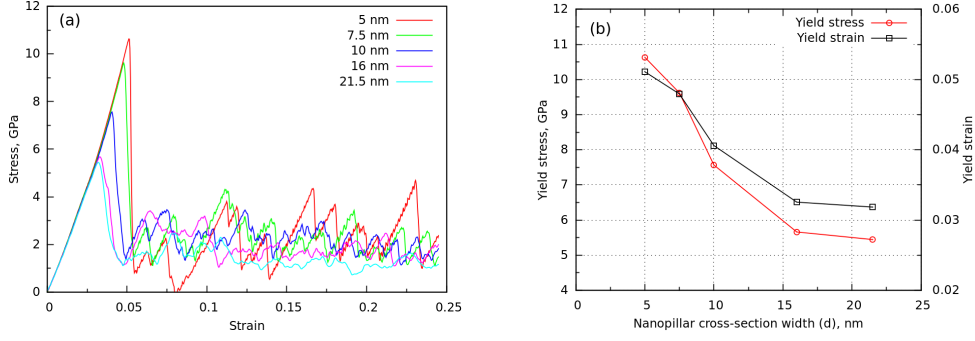


Figure 2.: (a) The stress-strain behaviour of $\langle 110 \rangle$ oriented Cu nanopillars with cross-section width (d) ranging from 5 - 21.5 nm under compressive loading. (b) The variation of yield stress and yield strain as a function of nanopillar size.

3. Results and Discussion

3.1. Stress-strain behaviour

The compressive stress-strain behaviour of $\langle 110 \rangle$ oriented Cu nanopillars with cross-section width (d) ranging from 5 - 21.5 nm is presented in Figure 2a at 10 K. It can be seen that all the nanopillars show similar stress-strain behaviour during the elastic deformation with an elastic modulus of 115 GPa. This value is in close agreement with experimental studies where the Young's modulus of $\langle 110 \rangle$ Cu falls in the range 121-138 GPa [27]. Following the elastic deformation up to the peak, the flow stress drops abruptly to low level of stress indicating the occurrence of yielding in the nanopillars. Post yielding, large flow stress oscillations were observed for nanopillars with $d = 5$ to 10 nm, while these oscillations were minimal in magnitude for nanopillars with $d = 16$ and 21.5 nm. Moreover, most of these oscillations were of saw tooth type and self similar, i.e., similar to the initial stress-strain curve up to yielding. Figure 2a also suggest that the yield strength as well as the yield strain varies significantly with nanopillar size. The variation of compressive yield stress as well as yield strain as a function of nanopillar size is plotted in Figure 2b. It shows that with increasing size, the yield stress (y_s) and yield strain of the Cu nanopillars decreases rapidly for smaller nanopillars followed by marginal decrease at large sizes. The variation of yield stress as a function of nanopillar size (d) obeys the power law relation $y_s = md^{-k}$, with $m = 24.5$ and exponent (k) = 0.50. The observed values of the exponent (k) are in the range that has been reported experimentally for micron sized FCC pillars (0.3 - 1) [28].

3.2. Deformation mechanisms

In order to reveal the deformation mechanisms, the evolution of atomic configurations at various stages of deformation were analyzed for all the nanopillars. It has been observed that the deformation is dominated by the slip of extended dislocations and no twinning was noticed. Figure 3a-b shows the typical yielding and subsequent plastic deformation behaviour of $\langle 110 \rangle$ oriented Cu nanopillars with $d = 21.5$ nm under compressive loading. It can be seen that the nanopillar yields on two different slip planes, α and β by the nucleation of a leading partial immediately followed by trailing partial on the same slip plane (Figure 3a). The combination of leading and trailing partial dislocations separated by a stacking fault constitutes an extended dislocation,

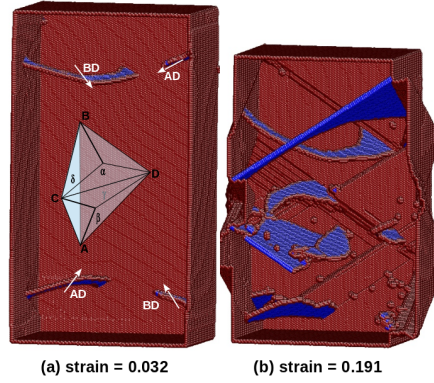


Figure 3.: The yielding (a), and subsequent plastic deformation behaviour (b), of $\langle 110 \rangle$ oriented Cu nanopillars with $d = 21.5$ nm under compressive loading. The Thompson tetrahedron is shown in (a) to identify the slip systems. The atoms are colored according to the common neighbor analysis. The perfect fcc atoms are removed for clarity and atoms on stacking faults are shown in blue, while those of dislocations and surface are shown in red.

AD and BD. In an extended dislocation, a trailing partial erases the stacking fault produced by the glide of leading partial. With increasing strain, more and more such dislocations nucleate on different $\{111\}$ planes (mainly α and β) and interact with each other. The typical dislocation-dislocation interactions leading to the formation of many point defects are shown in Figure 3b. The occurrence of full slip and the absence of twinning during the compressive loading of $\langle 110 \rangle$ nanopillar can be understood by the Schmid factor analysis [3,4,29]. According to this analysis, the Schmid factor of trailing partial (0.471) is higher than the leading partial (0.235), which leads to easy nucleation of trailing partials in the nanopillar. Since the trailing partials cannot nucleate without the leading partials, the nucleation of leading partials automatically proceeds the trailing partials leading to an occurrence of full slip through two consecutive partial slips on the same $\{111\}$ plane.

3.3. Size effects and dislocation starvation

MD simulations on nanopillars with other sizes, i.e., $d = 5, 7.5, 10$ and 16 nm indicated that the yielding and the subsequent plastic deformation is dominated by the slip of extended dislocations. However, few important differences were observed during the plastic deformation of nanopillars with smaller sizes. Since the probability of dislocation interactions within the nanopillar decreases with decreasing size, the dislocations gliding on the slip plane easily escape to surface and leads to easy dislocation starvation in small size nanopillars. Figures 4a-b show the typical snapshots displaying the state of perfect dislocation starvation and dislocation starvation with a wide stacking fault during the plastic deformation of nanopillar with $d = 10$ nm. Apart from starvation, many slip traces produced by the dislocations can also be seen on the surface of the nanopillar.

In order to find the frequency of occurrence of dislocation starvation and also its contribution to plastic strain, the number of stacking fault atoms were measured as a function of strain for all the nanopillars. Since the deformation is dominated by the

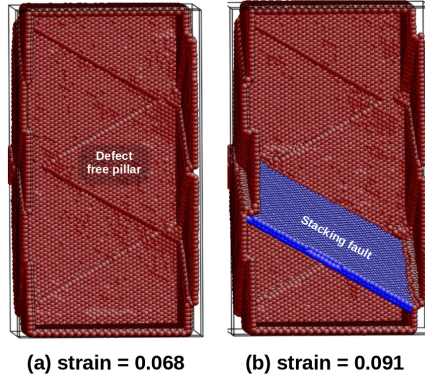


Figure 4.: The typical snapshots displaying the state of perfect dislocation starvation (a), and dislocation starvation with a wide stacking fault (b), during the plastic deformation of Cu nanopillar with $d = 10$ nm. The color coding of atoms is same as in Figure 3.

extended dislocations (partial dislocations separated by stacking faults), the absence of stacking fault atoms and/or zero change in the stacking fault atoms over a period of strain indicates dislocation starvation in the nanopillar (Figure 5). It can be seen that whenever the dislocation density is zero, i.e., dislocation starvation, the stacking fault atoms were either absent (zero) or constant. This suggest that the variation in % SF atoms can be used to identify the dislocation starvation events in the nanopillars. Unlike dislocation density, the calculation of % SF atoms requires minimal data and computation time, thus avoiding a tedious post-processing. Figures 6a-c show the percentage of stacking fault atoms along with flow stress as a function of strain for the nanopillars with $d = 7.5$, 10 and 21.5 nm, respectively. The dislocation starvation state is identified with blue arrow marks. It can be seen that for the nanopillar with $d = 7.5$ nm, the state of dislocation starvation occurs more frequently and each state occurring over extended period of strain (Figure 6a). With increasing the nanopillar size, the frequency of occurrence of dislocation starvation along with the duration of each state decreases (Figure 6b) and finally negligible dislocation starvation is observed in the nanopillar with $d = 21.5$ nm (Figure 6c). Further, it can be seen that when the nanopillar is in dislocation starvation state, the flow stress increases linearly indicating that the nanopillar undergoes repeated elastic deformations due to frequent dislocation starvation [14]. As a result of dislocation starvation, the strength of the nanopillar increases significantly.

3.4. Dislocation starvation strain

In order to characterize the contribution of dislocation starvation to the plastic strain or in turn plastic deformation, the aggregate strain over which the dislocation starvation occurs during the plastic deformation is measured for all the nanopillar sizes. This is obtained by combining the strain duration corresponding to the each arrow mark shown in Figure 6. Henceforth, this strain is termed as dislocation starvation strain. The value of dislocation starvation strain varies from 0.14 in nanopillar with $d = 5$ nm to a negligible 0.01 in nanopillar with $d = 21.5$ nm. However, the dislocation starvation strain alone may not be a useful parameter. To obtain the contribution of

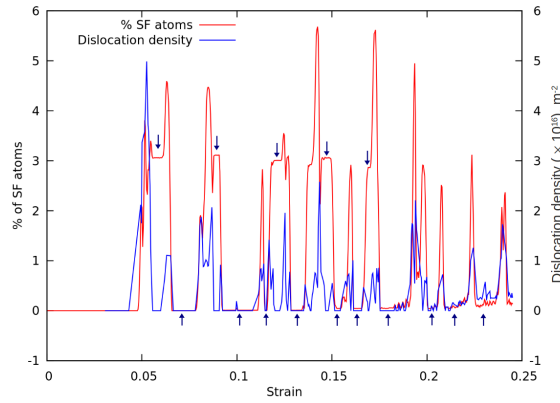


Figure 5.: The variation of percentage of stacking fault atoms along with dislocation density as a function of strain in the nanopillar with $(d) = 7.5$ nm. The short blue arrow marks indicates the dislocation starvation state, where the dislocation density is zero and the stacking fault atoms were either absent (zero) or constant.

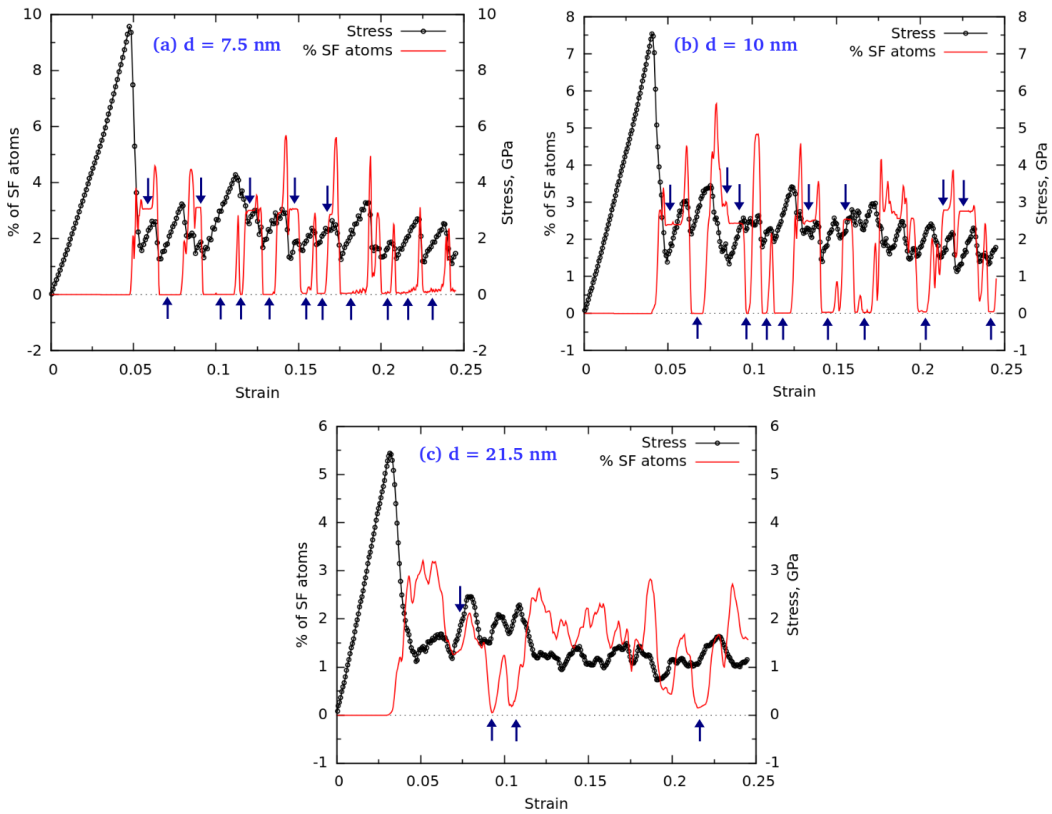


Figure 6.: The variation of percentage of stacking fault atoms along with flow stress as a function strain for the nanopillars with (a) $d = 7.5$ nm, (b) $d = 10$ nm, and (c) $d = 21.5$ nm. The short blue arrow marks indicates the dislocation starvation state.

dislocation starvation to the plastic strain, the ratio of dislocation starvation strain to that of the plastic strain is calculated as a function of nanopillar size and presented in Figure 7. It can be seen that the ratio decreases from 0.7 to 0.05, when the size increased from 5 nm to 21.5 nm. This indicates that for nanopillar with $d = 5$ nm, over 70% of the duration of the plastic deformation is spent in dislocation starvation state. The duration of dislocation starvation state decreases with increasing size and reduces to below 5% for the nanopillar with $d = 21.5$ nm (Figure 7). This suggest the existence of a threshold cross-section width of about 20 nm above which the dislocation starvation is almost negligible, ie., doesn't occur. Recently, in nanopillars of high entropy alloys, the critical size for the occurrence of dislocation starvation state is found to be around 15 nm and in perfect Cu nanopillars it is found to be close to 30 nm [30]. These results confirm that there exists a length scale in nanopillars below which the dislocation starvation can be observed. The main reasons for the observation of dislocation starvation in small size pillars is high image forces on dislocations coupled with less travel distance leading to easy escape of dislocations to the nearby free surfaces [7,10]. On the other hand, the small image forces along with longer travel distance increase the probability of dislocation interaction and multiplication resulting in nanopillars with large size populated with dislocations all the time [7,10]. Further, when the nanopillar is in dislocation starvation state, it deforms elastically even during the plastic deformation until new dislocations nucleate from the surfaces. This leads to the observation of saw tooth type large flow stress oscillations in small size nanopillars as shown in Figure 2a. Conversely, a negligible dislocation starvation in large size nanopillars caused minimal stress oscillations as seen from Figure 2a.

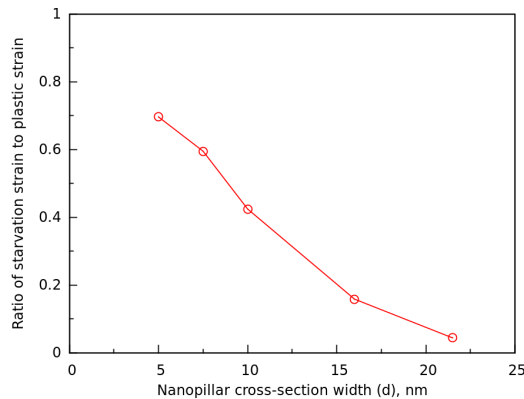


Figure 7.: The variation of the ratio of dislocation starvation strain to that of the plastic strain as a function of nanopillar size.

3.5. Dislocation starvation and twinning

The present results indicate that the $\langle 110 \rangle$ Cu nanopillars which deform by an extended dislocation slip exhibit an extensive dislocation starvation mechanism especially in small size pillars with $d < 20$ nm. In this context, it is interesting to understand the possibility of dislocation starvation when the nanopillar deforms by twinning mechanism. Since $\langle 110 \rangle$ oriented FCC nanopillars are expected to deform by twinning under tensile loading [4,29], additional MD simulations have been carried out on the tensile loading $\langle 110 \rangle$ Cu nanopillars with size $d = 10$ nm. The results indicate

that the deformation proceeds extensively by deformation twinning on two different twin systems (Figures 8a-b). The twin grows by the repeated nucleation and glide of twinning partials on twin boundaries. Compared to trailing partial nucleation which is required for extended dislocation slip, the nucleation of twinning partials require low stress [31,32]. As a result, a new twinning partial nucleate before the annihilation of the existing one, i.e., there is a continuous supply of twinning partials. Due to this, the twin boundaries are always populated with twinning partials and the dislocation starvation is rarely observed in case of nanopillars deforming by twinning mechanism (Figure 8). Due to the absence of dislocation starvation, the flow stress during the plastic deformation of nanopillar deforming by twinning shows no significant saw-tooth type fluctuations [19,29] in contrast to that shown in Figure 2a. These results show that the $\langle 110 \rangle$ Cu nanopillars exhibit tension-compression asymmetry in deformation mechanism as well as in dislocation starvation. The other important aspect of dislocation starvation is that it is observed mainly in FCC nanopillars. The dislocation starvation mechanism has not been observed in BCC nanopillars [13,33]. The high mobility coupled with a planer core structure enables easy escape of the dislocations to surfaces leading to dislocation starvation state in FCC nanopillars. Whereas in BCC nanopillars, the dislocations self multiply themselves before their annihilation [13,34] as result of which, the nanopillars are always populated with dislocations without any starvation.

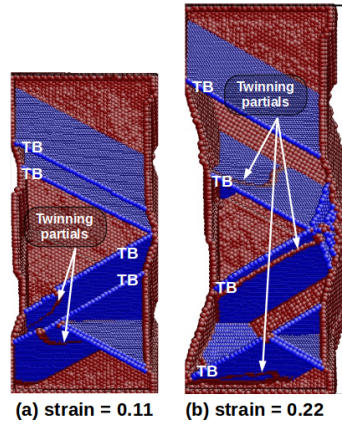


Figure 8.: The deformation behaviour of $\langle 110 \rangle$ Cu nanopillars with $d = 10$ nm under tensile loading. The deformation proceeds by twinning mechanism and the twin boundaries are always populated with twinning partials during twin growth, i.e., plastic deformation stage.

3.6. Effect of temperature, strain rate and stacking fault energy

Since the dislocation starvation is mainly due to the easy escape of dislocations to the surface, it is interesting to understand how the temperature, strain rate and stacking fault energy (SFE) influences the dislocation starvation mechanism in nanopillars. In nanoscale materials with high SFE, a pronounced dislocation starvation is reported [35]. The high SFE suppresses the dissociation of full dislocations into partials and hence results in easy escape of dislocations to the surface. Previous MD simulation study on $\langle 100 \rangle$ Cu nanowires has shown that for a given size, the exhaustion rates of

dislocations increases with increasing temperature and strain rate [36]. In other words, due to high velocity, the dislocations can easily escape to surface at high temperature and strain rates [37,38]. As a result, the nanopillar can easily go to dislocation starvation state. In contrast to this observation in Cu nanopillars, the dislocation dynamics (DD) simulations study on BCC Nb micropillars has shown that the suppression of thermally activated cross-slip at low temperatures prevents dislocation multiplication and thus results in easy dislocation starvation [39]. These contrasting observation in nanopillars and micropillars indicate that the effect of temperature on dislocation starvation in metallic nanopillars needs a detailed investigation. Apart from these factors, it will also be interesting to explore the effect of twin boundaries, which act as a strong obstacle to dislocation motion, on dislocation starvation.

4. Conclusions

Atomistic simulations have been performed to understand the size effects on the dislocation starvation mechanism in Cu nanopillars under compressive loading. Based on this study, the following conclusions have been drawn:

(1) The $\langle 110 \rangle$ Cu nanopillars with size (d) ranging from 5 to 21.5 nm deform by the slip of an extended dislocations and exhibit dislocation starvation mainly in small size nanopillars with $d < 20$ nm.

(2) The frequency of the occurrence of dislocation starvation state is highest in small size nanopillar with $d = 5$ nm and it decreases with increasing nanopillar size. Above 20 nm size, no incident of dislocation starvation has been observed.

(3) The dislocation starvation strain has been defined in this study and based on this, the contribution of dislocation starvation to the total plastic strain or plastic deformation is characterized. The contribution of dislocation starvation state to the total plastic strain is measured in terms of the ratio of dislocation starvation strain to that of the plastic strain. This ratio decreases from 0.7 to 0.05 when the size is varied from 5 nm to 21.5 nm. This indicates that for nanopillar with $d = 5$ nm, over 70% of the duration of the plastic deformation is spent in dislocation starvation state. This duration of dislocation starvation state decreases with increasing size and reduces to below 5% for the nanopillar with $d = 21.5$ nm.

(4) The variation of yield stress (y_s) as a function of nanopillar size (d) obeys the power law relation $y_s = md^{-k}$, with $m = 24.5$ and exponent (k) = 0.50.

(5) The dislocation starvation is not observed even in small size nanopillars when the deformation is dominated by twinning mechanism. This suggest that the dislocation starvation is a dominant phenomena when the deformation is dominated by the slip of partial/extended dislocations.

Disclosure statement

The authors report that there are no competing interests to declare.

Funding

This work received no funding.

Data availability

The data that support the findings in this paper are available from the corresponding author on request.

References

- [1] M.D. Uchic, D.M. Dimiduk, J.N. Florando, and W.D. Nix, Sample dimensions influence strength and crystal plasticity, *Science* 305 (2004) 986-989.
- [2] S.H. Oh, M. Legros, D. Kiener, P. Gruber, G. Dehm, In situ TEM straining of single crystal Au films on polyimide: Change of deformation mechanisms at the nanoscale, *Acta Mater.* 55 (2007) 5558-5571.
- [3] H.S. Park, K. Gall, and J.A. Zimmerman, Deformation of FCC nanowires by twinning and slip, *J. Mechan. Phys. Solids* 54 (2006) 1862-1881.
- [4] C.R. Weinberger and W. Cai, Plasticity of metal nanowires, *J. Mater. Chem.* 22 (2012) 3277-3292.
- [5] Y. Yue, P. Liu, Q. Deng, E. Ma, Z. Zhang, and X. Han, Quantitative evidence of cross-over toward partial dislocation mediated plasticity in copper single crystalline nanowires, *Nano Lett.* 12 (2012) 4045-4049.
- [6] D. Kong, S. Sun, T. Xin, L. Xiao, X. Sha, Y. Lu, S. Mao, J. Zou, L. Wang, and X. Han, Reveal the size effect on the plasticity of ultra-small sized Ag nanowires with in situ atomic-scale microscopy, *J. Alloys Compd.* 676 (2016) 377-382.
- [7] J.R. Greer and W.D. Nix, Nanoscale gold pillars strengthened through dislocation starvation, *Phys. Rev. B* 73 (2006) 245410.
- [8] Z.W. Shan, R.K. Mishra, SaS Asif, O.L. Warren, A.M. Minor, Mechanical annealing and source-limited deformation in submicrometre diameter Ni crystals, *Nature Mater.* 7 (2008) 115-119.
- [9] M. Kiritani, Dislocation-free plastic deformation under high stress, *Mater. Sci. Eng. A* 350 (2003) 1-7.
- [10] W.D. Nix, J.R. Greer, G. Feng, E.T. Lilleodden, Deformation at the nanometer and micrometer length scales: Effects of strain gradients and dislocation starvation, *Thin Solid Films* 515 (2007) 3152 - 3157.
- [11] C. Griesbach, J. Seog-Jin, D.F. Rojas, M. Ponga, S. Yazdi, S. Pathak, N. Mara, E.L. Thomas, R. Thevamaran, Origins of size effects in initially dislocation-free single-crystal silver micro-and nanocubes, *Acta Mater.* 214 (2021) 117020.
- [12] J.R. Greer, C.R. Weinberger, W. Cai, Comparing the strength of fcc and bcc sub-micrometer pillars: Compression experiments and dislocation dynamics simulations, *Mater. Sci. Eng. A*, 493 (2008) 21-25.
- [13] C.R. Weinberger and W. Cai, Surface-controlled dislocation multiplication in metal micropillars, *Proc. Natl. Acad. Sci. U. S. A.* 105 (2008) 14304.
- [14] A. Cao, Y. Wei and S.X. Mao, Alternating starvation of dislocations during plastic yielding in metallic nanowires, *Scr. Mater.* 59 (2008) 219-222.
- [15] C. Zhou, B. Biner, R. LeSar, Discrete dislocation dynamics simulations of plasticity at small scales, *Acta Mater.* 58 (2010) 1565-1577.
- [16] S.J. Plimpton, Fast parallel algorithms for short-range molecular dynamics, *J. Comput. Phys.* **117** (1995) 1-19.
- [17] Y. Mishin, M.J. Mehl, D.A. Papaconstantopoulos, A.F. Voter, and J.D. Kress, Structural stability and lattice defects in copper: Ab initio, tight-binding, and embedded-atom calculations, *Phys. Rev. B* **63**, 1 (2001).
- [18] H. Liang, M. Upmanyu, and H. Huang, Size-dependent elasticity of nanowires: Nonlinear effects, *Phys. Rev. B* 71 (2005) 241403.
- [19] G. Sainath and B.K. Choudhary, Molecular dynamics simulation of twin boundary effect

- on deformation of Cu nanopillars, *Phys. Lett. A* 379 (2015) 1902-1905.
- [20] D. Zhang, R. Wang, M. Wen, D. Weng, X. Cui, J. Sun, H. Li, Y. Lu, Synthesis of Ultralong Copper Nanowires for high-performance transparent electrodes, *J. Am. Chem. Soc.* 134 (2012) 14283- 14286.
- [21] S. Xu, Y.F. Guo, A.H.W. Ngan, A molecular dynamics study on the orientation, size, and dislocation confinement effects on the plastic deformation of Al nanopillars, *Inter. J. Plast.* 43 (2013) 116-127
- [22] G. Sainath, Sunil Goyal, A. Nagesha, Atomistic mechanisms of twin-twin interactions in Cu nanopillars, *Comput. Mater. Sci.* 185 (2020) 109950.
- [23] J.A. Zimmerman, E.B. Webb, J.J. Hoyt, R.E. Jones, P.A. Klein, and D.J. Bammann, Calculation of stress in atomistic simulation, *Modell. Simul. Mater. Sci. Eng.* 12 (2003) S319.
- [24] J. Li, AtomEye: An efficient atomistic configuration viewer, *Modell. Simul. Mater. Sci. Eng.* 11 (2003) 173-177.
- [25] A. Stukowski and K. Albe, Dislocation detection algorithm for atomistic simulations, *Modell. Simul. Mater. Sci. Eng.* 18 (2010) 025016.
- [26] A. Stukowski, Visualization and analysis of atomistic simulation data with OVITO - The Open Visualization Tool, *Modell. Simul. Mater. Sci. Eng.* 18 (2009) 015012.
- [27] D.E.J. Armstrong, A.J. Wilkinson, S.G. Roberts, Measuring anisotropy in Young's modulus of copper using microcantilever testing, *J. Mater. Res.* 24 (2009) 3268-3276
- [28] R. Gu, A.H.W. Ngan, Dislocation arrangement in small crystal volumes determines power-law size dependence of yield strength, *J. Mech. Phys. Solids.* 61 (2013) 1531-42.
- [29] P. Rohith, G. Sainath, B.K. Choudhary, Effect of orientation and mode of loading on deformation behaviour of Cu nanowires, *Comput. Cond. Matter* 16 (2018) e00330.
- [30] L. Wang, B. Liu, J. Zhou, Y. Cao, F. Zhang, Y. Zhao, Unconventional dislocation starvation behavior of medium-entropy alloy single crystal pillars containing pre-existing dislocations, *J. Mater. Sci. Tech.* 142 (2023) 60-75.
- [31] J.-H. Seo, H.S. Park, Y. Yoo, T.-Y. Seong, J. Li, J.-P. Ahn, B. Kim, I.-S. Choi, Origin of size dependency in coherent-twin-propagation-mediated tensile deformation of noble metal nanowires, *Nano Lett.* 13 (2013) 5112-5116.
- [32] A. Cao, Shape memory effects and pseudoelasticity in bcc metallic nanowires *J. Appl. Phys.* 108 (2010) 113531.
- [33] G. Sainath, B.K. Choudhary, Molecular dynamics simulations on size dependent tensile deformation behaviour of [110] oriented body centred cubic iron nanowires, *Mater. Sci. Eng. A* 640 (2015) 98-105
- [34] G. Sainath, B.K. Choudhary, Atomistic simulations on ductile-brittle transition in $\langle 111 \rangle$ BCC Fe nanowires, *J. Appl. Phys.* 122 (2017) 095101.
- [35] F. Duan, Q. Li, Z. Shen, Z. Jiang, W. Liu, Y. Yan, J. Pan, L. Sun, J. Lu, Anisotropic mechanical properties and deformation mechanisms of nanotwinned Ni and Ni alloys with extremely fine twin boundary spacings, *Acta Mater.* 260 (2023) 119311.
- [36] P. Rohith, G. Sainath, V.S. Srinivasan, Effect of size, temperature and strain rate on dislocation density and deformation mechanisms in Cu nanowires, *Physica B: Cond. Matter* 561 (2019) 136-140.
- [37] A.P.L. Turner, T. Vreeland Jr., The effect of stress and temperature on the velocity of dislocations in pure iron monocrystals, *Acta Metall.* 18 (1970) 1225.
- [38] G.E. Dieter, D.J. Bacon, *Mechanical Metallurgy* vol. 3, McGraw-hill, New York, 1986
- [39] G. Song, N.K. Aragon, I. Ryu, S.-W. Lee, Low-temperature failure mechanism of [001] niobium micropillars under uniaxial tension, *J. Mater. Res.* 36 (2021) 2371-2382.